Santhi Sheela Yerraguntla, Haladhara Naik*, Manjunatha Karantha, Srinivasan Ganesan, Suryanarayana Venkata Saraswatula and Sreekumaran Narayana Pillai Nair

Measurement and covariance analysis of ^{59}Co(n, 2n)^{58}Co reaction cross sections at the effective neutron energies of 11.98 and 15.75 MeV

https://doi.org/10.1515/ract-2018-2937
Received February 6, 2018; accepted May 30, 2018; published online July 14, 2018

Abstract: The ^{59}Co(n, 2n)^{58}Co reaction cross sections relative to the cross sections of the ^{115}In(n, n')^{115m}In reaction have been measured at the effective neutron energies of 11.98 and 15.75 MeV by using activation and off-line γ-ray spectrometric technique. Neutron beam used in the present experiment was generated from the ^{7}Li(p, n)^{7}Be reaction with the proton energies of 14 and 18 MeV at the 14UD BARC-TIFR Pelletron facility, Mumbai. We also present the covariance information by taking into account the sources of error and the correlations between the attributes influencing the measurements. The ^{59}Co(n, 2n)^{58}Co reaction cross sections from the present work are then compared with the values from different evaluated nuclear data libraries. The micro-correlation technique suggested by Smith was modified to generate the covariance matrix for the measurements of reaction cross sections as the efficiencies of detector for the sample and monitor are correlated.

Keywords: ^{59}Co(n, 2n)^{58}Co cross section, neutron activation, off-line γ-ray spectrometry, EXFOR, IRDFF-1.05, evaluated data libraries, covariance analysis.

***Corresponding author: Haladhara Naik,** Radiochemistry Division, Bhabha Atomic Research Centre, Mumbai-400085, India, E-mail: naikhbarc@yahoo.com
Santhi Sheela Yerraguntla and Manjunatha Karantha: Department of Statistics, PSPH, MAHE, Manipal, Karnataka-576104, India
Srinivasan Ganesan: Former Raja Ramanna Fellow of DAE, Bhabha Atomic research Centre, Mumbai-400085, India
Suryanarayana Venkata Saraswatula: Nuclear Physics Division, Bhabha Atomic Research Centre, Mumbai-400085, India
Sreekumaran Narayana Pillai Nair: Department of Biostatistics (Biometrics), JIPMER, Puducherry, Tamilnadu 605 006, India

1 Introduction

The neutron-induced reaction cross sections are important for different applications such as industrial production of radioisotopes, the design of conventional reactors and Accelerator-Driven Sub-critical systems (ADSs). The reaction cross section data in the higher neutron energy region are relevant to ADSs [1]. The cross sections of reactions such as (n, γ), (n, n'), (n, p), (n, α) and (n, 2n) reactions of structural materials are important from the point of view of neutron economy of the thermal and fast neutron reactors, and thus are needed for advanced reactor designs. This is because the neutron energies in conventional and advanced reactors vary from 0.025 eV to 20 MeV. The neutron induced reaction cross sections data are of practical application in fusion reactor technology, particularly for calculations on tritium breeding, gas production in structural materials and activation of reactor components [2–5]. In particular, the above mentioned nuclear reactions lead to the formation of hydrogen and helium gases in the reactor wall at different locations. The important structural materials for reactors are zirconium, niobium, stainless steel and aluminum. In reactor, stainless steel is used in the calandria vessel and pipe lines of the secondary coolant circuit. Stainless steel is constituted of natural iron with different percentages of Cr, Mn, Co and Ni. Different neutron induced reaction cross sections of structural materials have been measured by various authors [2–5]. In particular Qaim [3] has shown the systematics of (n, 2n) reaction cross sections around the neutron energies of 14–15 MeV. He found that the (n, 2n) reaction cross section at 14 MeV is low for light mass nuclei and increases rapidly with the increasing neutron excess of the target nucleus. On the other hand, Bostan and Qaim [5] have shown that the excitation function of the (n, 2n) reaction shows a rapid increase in the energy region between 10 and 14 MeV. In view of all the above facts, the measurement of (n, 2n) reaction cross section of ^{59}Co has been chooosen in the present work.

The measurements of ^{59}Co(n, 2n)^{58}Co reaction cross sections at different neutron energies between 10 and

20 MeV have been reported by various authors [6–22] using neutron activation method and different counting techniques. In all the cases neutrons were produced either via the D + D reaction or the D + T reaction, and the measurements above the neutron energy of 13.8 MeV found in literature are rather limited and scattered. Therefore, in the present work, the ^{59}Co(n, $2n$)^{58}Co reaction cross sections relative to the ^{115}In(n, n')^{115m}In monitor reaction have been measured at two effective neutron energies of 11.98 and 15.75 MeV (i. e. on both sides of 13.8 MeV). The neutron beams were generated from the ^{7}Li(p, n) reaction by using proton beams of 14 and 18 MeV. Covariance analysis of the uncertainties in the cross sections was performed by taking into account every source of error and the correlations between the attributes influencing the error in the measurements. The ^{59}Co(n, $2n$)^{58}Co reaction cross section and its covariance analysis are important for Indian nuclear power programme [23]. The present data were compared with the values of evaluated nuclear data libraries [24–30].

2 Experimental details

The experiment was performed by using the 14UD BARC-TIFR, Pelletron facility at Mumbai, India. The neutron beam was produced using the ^{7}Li(p, n)^{7}Be reaction from the proton main line at 6 m above the analyzing magnet of the Pelletron facility to utilize the maximum proton current from the accelerator. At this port, the terminal voltage is regulated by generating voltage mode (GVM) by using a terminal potential stabilizer. Further a collimator of 6 mm diameter was used before the lithium target. The protons of beam energies 14 and 18 MeV were used to bombard a natural lithium (Li) target kept inside a Tantalum–Lithium–Tantalum (Ta–Li–Ta) stack to generate the neutrons. The lithium foil was made up of natural lithium with thickness 3.7 mg/cm^2, and the two tantalum foils were of different thicknesses. The front tantalum foil facing the proton beam was the thinner one (3.9 mg/cm^2), in which the degradation of proton energy, according to the SRIM [31] was 48–58 keV. The back tantalum foil of thickness more than 0.025 mm was used to stop the proton beam.

Two Co metal foils of radius 0.25 cm and 0.3 cm were wrapped separately with Al foil of thickness 0.025 mm. Similarly, In metal foils of size 0.5 cm × 0.6 cm and 0.8 cm × 0.6 cm were separately wrapped with Al foil of same thickness to prevent radioactive contamination during irradiation. Two sets of Al wrapped cobalt and two sets of Al wrapped indium were used to make two stacks for the irradiation purpose. The individual stacks of Co-In were additionally wrapped with Al foils. The stacks were then mounted one at a time in 0^0 angle with respect to the proton beam direction at a distance of 2.1 cm behind the Ta–Li–Ta stack. A schematic diagram of the experimental arrangement can be found in Ref. [32].

The stacks were irradiated one after other with effective neutron energies of 11.98 and 15.75 MeV. The discussion on effective neutron energies $E_n = 11.98 \pm 0.29$, 15.75 ± 0.31 MeV is given in Ref. [33]. The corresponding irradiation times of the two stacks were 7 and 11.17 h, respectively. The irradiated cobalt foils from the two stacks were then allowed to decay for 22.8 and 12.4 h, respectively. Similarly, the corresponding irradiated indium foils were allowed to decay for 2.9 and 1.1 h, respectively. The irradiated cobalt and indium foils were then mounted separately on different Perspex plates. The γ-ray counting of the irradiated foils was done by using a pre-calibrated 80 cm^3 HPGe detector coupled to a PC-based 4094 channel analyser kept at a suitable distance from the detector cap to avoid the summation effect. The resolution of the detector system had a full-width at half-maximum of 2 keV at 1332.5 keV of ^{60}Co. The efficiency calibration as a function of energy was performed by using standard ^{152}Eu point source, maintaining the same geometry. Since the γ-ray counting of the standard ^{152}Eu point source was done in the same geometry at a suitable distance from the end cap of the detector, the summation effect was avoided. This has been tested by doing the γ-ray counting of the standard ^{241}Am, ^{137}Cs and ^{60}Co sources in the same geometry.

The γ-ray counting of the irradiated In and Co samples was done many times with increasing counting time and decay time to have good counting statistics and to follow the half-lives. Besides this, the radionuclide ^{58}Co has a metastable state with a half-life of 9.1 h, which dacys to the ground state by internal transition of 100 % branching intensity [4, 34]. Thus the γ-ray counting data, obtained after complete decay of ^{58m}Co to ^{58g}Co were used in calculation of the ^{59}Co(n, $2n$)^{58}Co reaction cross section.

3 Data analysis

The sample reaction cross section, which is to be measured, is usually derived with the help of a well-established monitor reaction cross section by considering their ratio given by the experimental observations. This method avoids the need of absolute neutron flux Φ, which is difficult to measure but is necessary in conventional computation of reaction cross section. The following expression was used in the ratio method to measure the sample reaction cross section.

$$\sigma_U(E_n)=\sigma_M(E_n)\frac{C_U\lambda_U Wt_M abn_M Av_U\left(\frac{CL}{LT}\right)_U (I_\gamma)_M(\varepsilon(E_\gamma))_M(1-e^{-\lambda_M tirr_M})(e^{-\lambda_M twait_M})(1-e^{-\lambda_M tc_M})}{C_M\lambda_M Wt_U abn_U Av_M\left(\frac{CL}{LT}\right)_M (I_\gamma)_U(\varepsilon(E_\gamma))_U(1-e^{-\lambda_U tirr_U})(e^{-\lambda_U twait_U})(1-e^{-\lambda_U tc_U})}\prod_k\frac{(C_k)_M}{(C_k)_U} \quad (1)$$

where $\sigma_U(E_n)$ is the unknown cross section of ^{59}Co(n, 2n)^{58}Co reaction at the neutron energy E_n, $\sigma_M(E_n)$ is the known cross section of the ^{115}In(n, n')^{115m}In monitor reaction at the neutron energy E_n, C_U, λ_U, $(I_\gamma)_U$, $(\varepsilon(E_\gamma))_U$ are the detected γ-ray counts, the decay constant of product nuclei, γ-ray abundances and the efficiencies of the detector corresponding to characteristic γ-rays of reaction products of ^{58}Co. Similarly, C_M, λ_M, $(I_\gamma)_M$, $(\varepsilon(E_\gamma))_M$ are the detected γ-ray counts, the decay constant of product nuclei, γ-ray abundances and the efficiencies of detector corresponding to characteristic γ-rays of reaction products ^{115m}In. The term $\left(\frac{CL}{LT}\right)_i$ with clock time, CL and live time, LT is for dead time effect correction. Wt_U, Wt_M are the weights of cobalt and indium foils respectively, abn_U, Av_U are the isotopic abundances and the average atomic mass of ^{59}Co. Similarly, abn_M, Av_M are the isotopic abundances and average atomic mass of ^{115}In. *tirr*, *twait* and *tc* are the irradiation time, waiting time and counting time of the samples, respectively. $(C_k)_U$, $(C_k)_M$ are the correction factors which include correction factor due to area of the foils A_i and lastly the correction factor α_i accounting for the low energy neutron contribution. It may be noted that

$$\alpha_i=\left(1+\frac{\sum_{p_2}\Phi(E_{P_2})\sigma_i(E_{P_2})+\int_0^{E_{max}}\varphi(E)\sigma_i dE}{\sum_{p_1}\Phi(E_{P_1})\sigma_i(E_{P_1})}\right),\ i=U,\ M \quad (2)$$

where Φ represents the flux corresponding to discrete peaks, and φ is the continuum with reference to the neutron spectra. The terms E_{P_1}, E_{P_2} in Eq. (2) represent the neutron energies corresponding to higher and lower energy neutron peaks. E is the neutron energy, which corresponds to much lower energy tail part of the neutron spectra. $\sum_{p_1}, \sum_{p_2}$ indicates add up all the number of groups under higher and lower peak. The correction term α_i in Eq. (2) was obtained by following the approach of Smith et al. [35]. The self-attenuation factor (g_{attn}) of the foil was determined using the expression [36], $g_{attn}=\frac{1-e^{-\mu L}}{\mu L}$, where L is the thickness of the sample and μ is mass attenuation coefficient obtained using XMuDat Ver. 1.01 [37].

The neutron spectra in the ^{7}Li(p, n)^{7}Be reaction for the proton enrgies of 14 and 18 MeV have tail parts besides the peak neutron energies, which can be seen from Ref. [32]. The threshold energy of the ^{115}In(n, n')^{115m}In monitor reaction is 0.5 MeV, whereas that of the ^{59}Co(n, 2n)^{58}Co reaction, it is 8.3 MeV. So it is necessary to take care of the contribution in the neutron flux and the flux-weighted reaction cross section due to the tail part of the neutron spectrum as well as different threshold values of the ^{115}In(n, n')^{115m}In monitor reaction and ^{59}Co(n, 2n)^{58}Co reaction [32]. This was taken care by using the eq. (2) instead of finding the individual neutron flux and flux-weighted reaction cross section separately.

3.1 Energy and efficiency calibration of HPGe detector with covariance analysis

In this experiment, energy and efficiency calibration of HPGe detector was carried out using single standard point source ^{152}Eu. For this purpose, eight γ-ray energies were chosen. The experimental data (C) and auxiliary data (I_γ, A_0, $T_{1/2}$) were observed for each of these γ-ray energies and the same are presented in Table 1. With the information on uncertainty in each of these observations and the micro-correlations between them, efficiency vector of the detector $\vec{\varepsilon}=(\varepsilon_1, \varepsilon_2, .., \varepsilon_8)^T$ corresponding to these γ-ray energies and the relevant covariance information were obtained.

After completing the calibration process, a linear model $Z \approx AP$ was chosen to derive a suitable linear parametric function to obtain the efficiencies of the detector at characteristic γ-rays corresponding to the reaction

Table 1: Data on efficiency calibration of the detector using a ^{152}Eu source.

γ-Ray energy (MeV)	γ-Ray abundance (%)	Counts for 976 s	K_c	Efficiency
0.121782	28.53 ± 0.16	41243 ± 303	1.344	5.602E-02
0.244697	7.55 ± 0.04	5275 ± 114	1.547	3.116E-02
0.443961	2.827 ± 0.014	1144 ± 73	1.464	1.708E-02
0.488679	0.414 ± 0.003	131 ± 52	1.620	1.478E-02
0.688670	0.856 ± 0.006	257 ± 52	1.351	1.170E-02
0.964057	14.51 ± 0.07	2450 ± 70	1.415	6.889E-03
1.112076	13.67 ± 0.08	1898 ± 53	1.354	5.420E-03
1.408013	20.87 ± 0.09	2180 ± 50	1.378	4.150E-03

products ^{58}Co, ^{115m}In. The linear parametric function $\log \varepsilon = p_0 + p_1 \log E + p_2(\log E)^2$ with $p_0 = -5.040$, $p_1 = -1.295$ and $p_2 = -0.128$ was used as the best fit for the energy and efficiency model with corresponding $\frac{\chi^2}{8-3} = 0.57 \approx 1$. Further details on choosing the appropriate model, and step by step procedure of estimation of the efficiencies of the detector corresponding to characteristic γ-rays with a covariance analysis are available in Ref. [38]. Table 2 provides the results of efficiencies estimation with the corresponding correlation matrix.

3.2 Estimation of ^{59}Co(n, $2n$)^{58}Co reaction cross section with covariance analysis

Basic data (half-life, γ-ray abundance, and isotopic abundance) along with uncertainty information used in obtaining $\sigma_U(E_n)$ were retrieved from ENSDF data sets through NuDat web interface [34] maintained by National Nuclear Data Center (NNDC) and are presented in Table 3.

Applying the interpolation technique we obtain the cross section of the ^{115}In(n, n')^{115m}In monitor reaction at the effective neutron energies of 11.98, 15.75 MeV (IRDFF-1.05, [30]). Further to obtain covariance information, we refer to relative covariance information for the cross sections in the corresponding energy group available in the IRDFF-1.05 file, and then propagate the same to the monitor cross sections at the desired energies. The details of monitor cross section along with covariance and correlation matrices are given in Table 4.

The corresponding covariance information for $\sigma_U(E_n)$ with covariance matrix $V_{\sigma_U(E_n)}$ whose (i, j)th entry is given by

$$(V_{\sigma_U(E_n)})_{ij} = \sum_{kl} (e_k)_i, (e_l)_j (S_{kl})_{ij}, \; 1 \le i, j \le 2, \; 1 \le l, k \le 18, \quad (5)$$

where $(e_k)_i = \frac{\partial \sigma_U(E_n)_i}{\partial (x_k)_i} \Delta(x_k)_i$, is the partial uncertainty in $(\sigma_U(E_n))_i$ due to kth attribute and $(e_l)_j = \frac{\partial \sigma_U(E_n)_j}{\partial (x_l)_j} \Delta(x_l)_j$, is the partial uncertainty in $(\sigma_U(E_n))_j$ due to lth attribute. $(S_{kl})_{ij}$ is the correlation between kth attribute in the ith experiment and lth attribute in the jth experiment. Readers are referred to Appendix A of Ref. [39] for the detailed description of Eq. (5).

To compute $\sigma_U(E_n)$, the attributes considered are $\sigma_M(E_n)$, C_U, C_M, λ_U, λ_M, Av_M, Av_U, Wt_U, Wt_M, abn_M, $(I_\gamma)_U$, $(I_\gamma)_M$, $(\varepsilon(E_\gamma))_U$, $(\varepsilon(E_\gamma))_M$, A_U, A_M, $(g_{attn})_U$ and $(g_{attn})_M$. The terms *tirr*, *twait* and *tc* given in the Eq. (1) are observed without error and treated as constant. The partial uncertainties in $\sigma_U(E_n)$ due to each of the attributes mentioned above were obtained as described in Eq. (5) and presented in Table 5. The observations between any two attributes are independent of each other except for the pair of attributes $(\varepsilon(E_\gamma))_M$ and $(\varepsilon(E_\gamma))_U$, where the correlation between each of the observations of $(\varepsilon(E_\gamma))_M$ and the observations of $(\varepsilon(E_\gamma))_U$

Table 2: Efficiencies of the detector corresponding to energies of characteristic γ-rays and uncertainty matrix.

Radionuclide	γ-Ray energy (MeV)	Efficiency	Correlation matrix	
^{58}Co	0.81076	0.00845 ± 0.00017	1	0.87
^{115m}In	0.33624	0.0228 ± 0.00057	0.87	1

Table 3: Data required for estimating $\sigma_U(E_n)$.

Nuclide	Tag number	Weight (g)	Half-life	γ-ray abundance (%)	Isotopic abundance of target nuclide (%)
^{115m}In	In-1	0.0675 ± 0.0013	4.486 ± 0.004 h	45.9 ± 0.1	95.71 ± 0.05
	In-2	0.0737 ± 0.0015			
^{58}Co	Co-1	0.3800 ± 0.0076	70.86 ± 0.06 days	99.45 ± 0.01	100
	Co-2	0.2171 ± 0.0043			

Table 4: Monitor cross sections as obtained by interpolating the cross section data taken from IRDFF, along with covariance matrix and correlation matrix.

Neutron energy (MeV)	^{115}In(n, n')^{115m}In cross section (b)	Covariance matrix		Correlation matrix	
11.98 ± 0.29	0.1530 ± 0.0122	1.479E-04	6.301E-06	1	0.247
15.75 ± 0.31	0.0565 ± 0.002	6.301E-06	4.408E-06	0.247	1

Table 5: Partial uncertainties in $\sigma_U(E_n)$.

	Attributes	Partial uncertainties in ^{59}Co(n, 2n)^{58}Co		Correlation
		E_n = 11.98 (MeV)	E_n = 15.75 (MeV)	
Co	Gamma-ray counts C_U	2.73E-02	4.64E-02	Uncorrelated
	Decay constant λ_U	1.97E-04	6.13E-04	Fully correlated
	Average atomic mass Av_U	1.60E-08	4.96E-08	Fully correlated
	Weight of sample Wt_U	4.69E-03	1.46E-02	Uncorrelated
	Gamma-ray abundance $(I_\gamma)_U$	2.37E-05	7.34E-05	Fully correlated
	Efficiency of detector $(\varepsilon(E_\gamma))_U$ [b]	4.67E-03	1.45E-02	Fully correlated
	Correction factor for area A_U	4.54E-03	1.41E-02	Uncorrelated
	Correction factor for gamma-ray attenuation gattn$_U$	9.25E-05	1.93E-04	Uncorrelated
In	Monitor cross section $\sigma_M(E_n)$	1.87E-02	2.71E-02	Partially correlated[a]
	Gamma-ray counts C_M	4.15E-03	1.23E-02	Uncorrelated
	Decay constant λ_M	1.31E-05	1.05E-04	Fully correlated
	Average atomic mass Av_M	2.05E-06	6.36E-06	Fully correlated
	Weight of sample Wt_M	4.64E-03	1.47E-02	Uncorrelated
	Isotopic abundance abn_M	1.23E-04	3.81E-04	Fully correlated
	Gamma-ray abundance $(I_\gamma)_M$	5.14E-04	1.59E-03	Fully correlated
	Efficiency of detector $(\varepsilon(E_\gamma))_M$ [b]	5.84E-03	1.81E-02	Fully correlated
	Correction factor for area A_M	3.21E-03	9.93E-03	Uncorrelated
	Correction factor for gamma-ray attenuation gattn$_M$	3.86E-04	4.97E-04	Uncorrelated

[a]Correlation value is given in Table 4. [b]Cor $((\varepsilon(E_\gamma))_U, (\varepsilon(E_\gamma))_M) = 0.87$.

Table 6: ^{59}Co(n, 2n)^{58}Co reaction cross sections.

Neutron energy (MeV)	^{59}Co(n, 2n)^{58}Co cross section (b)	Covariance matrix		Correlation matrix	
11.98 ± 0.29	0.2358 ± 0.0368	0.00129	0.00045	1	0.18
15.75 ± 0.31	0.7301 ± 0.0687	0.00045	0.00476	0.18	1

are correlated, with correlation coefficient equal to 0.87 (refer to Table 2).

The observations of the attributes C_U, C_M, Wt_U, Wt_M, A_U, A_M, $(g_{attn})_U$ and $(g_{attn})_M$ with reference to different neutron energies are independent of each other and therefore the corresponding micro-correlation matrices are identical and equal to the identity matrix of order two. The correlation matrix of the measurements $\sigma_M(E_n)$ for different neutron energies will now be considered as the micro-correlation matrix associated with the attribute $\sigma_M(E_n)$ and the same was taken from Table 4.

The micro-correlation matrices associated with the attributes λ_U, λ_M, Av_U, Av_M, $(I_\gamma)_U$, $(I_\gamma)_M$, $(\varepsilon(E_\gamma))_M$ and $(\varepsilon(E_\gamma))_U$ are identical and equal to matrix of order two with all entries equal to one, as the same observation of attributes were used in different neutron energy cases. Substituting the partial uncertainties data presented in Table 5, and the above information of micro-correlations in Eq. (5), the elements of covariance matrix $V_{\sigma_U(E_n)}$ of $\sigma_U(E_n)$ were generated and the same are presented in Table 6.

4 Results and discussion

In the present work, the measurements of ^{59}Co(n, 2n)^{58}Co reaction cross sections and covariance analysis of their uncertainties were obtained relative to the standard cross sections of ^{115}In(n, n')^{115m}In reaction at the effective neutron energies of 11.98 and 15.75 MeV. The micro-correlation technique introduced by Smith [40] was modified to obtain the covariance information. The ^{59}Co(n, 2n)^{58}Co reaction cross sections from the present work and literature as well as the evaluated data of different nuclear data libraries such as JENDL 4.0 [27], CENDL 3.1 [25], JEFF 3.2 [28], ROSFOND 2010 [26], TENDL 2015 [41], and ENDF/B-VII.1) [24, 42] are plotted in Figure 1. It is observed that the cross section measured in the present experiment at the neutron energy of 11.98 MeV is in good agreement with all the evaluated data, but in the case of 15.75 MeV, the present measurement is comparatively lower than the evaluated data. It may be noted that the experimental data based on the D + T reaction are in good agreement with the

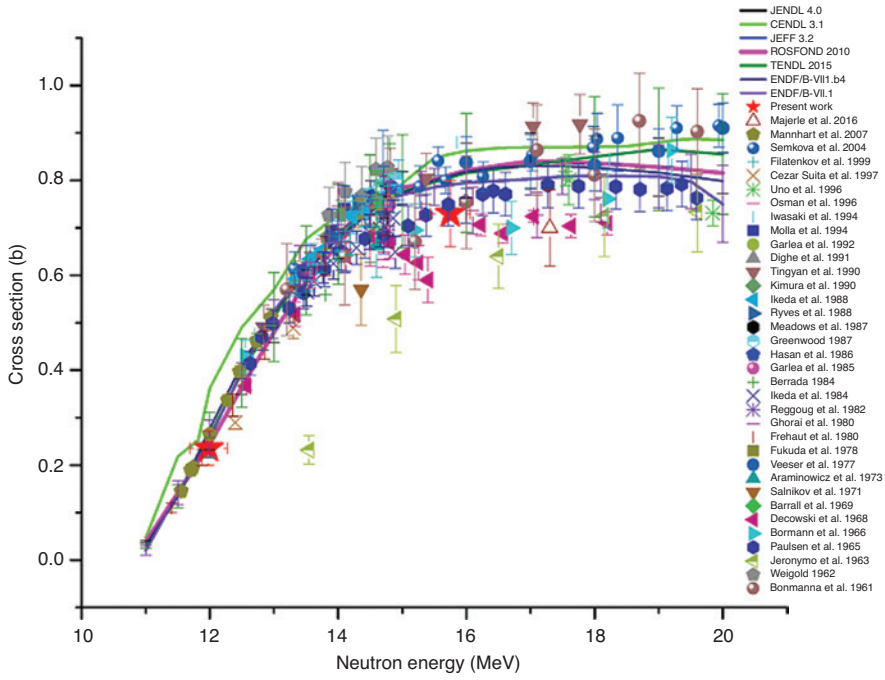

Figure 1: A plot showing the comparison of experimental ^{59}Co(n, 2n)^{58}Co reaction cross section from the present work at the effective neutron energies of 11.98 and 15.75 MeV with the literature data (for reference given on the right, see EXFOR [43]).

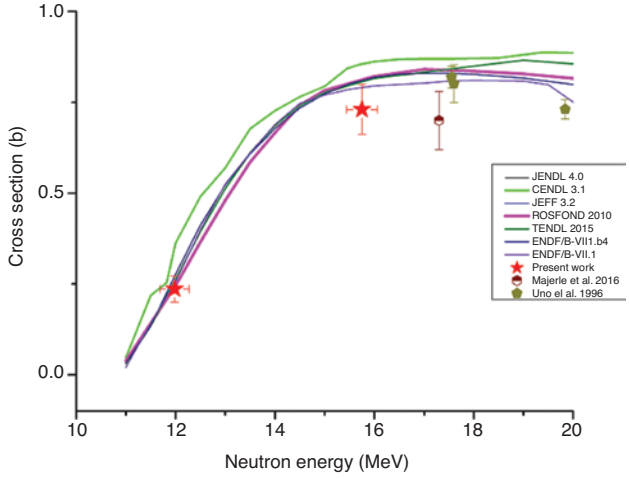

Figure 2: Comparison of experimental ^{59}Co(n, 2n)^{58}Co reaction cross section (barns) based on experiments using only the ^{7}Li(p, n) reaction (for reference given on the right, see EXFOR [43]).

evaluated data. However, the experimental data above the neutron energy of 15 MeV based on the ^{7}Li(p, n) reaction are below the evaluated data. In view of this, the experimental data from the present work and similar data from literature [14, 22] based on the ^{7}Li(p, n) reaction neutron sources are presented in Figure 2. It can be seen that the experimental data based on the ^{7}Li(p, n) reaction neutron sources around 15–20 MeV are lower than the evaluated data, which supports our present observation. The lower experimental value around the neutron energies of 15–20 MeV may be due to the use of quasi-mono energetic ^{7}Li(p, n) reaction neutrons and ^{115}In(n, n')^{115m}In reaction monitor, where correction for the neutron background may not be so perfect.

Further, it can be seen from Figures 1 and 2 that the data from different evaluations have slight variation. Ignoring the slight deviations, one can see from Figures 1 and 2 that the experimental and evaluated ^{59}Co(n, 2n)^{58}Co reaction cross section increases with neutron energy. However, the increase in trend is very fast from the threshold value to the neutron energy of 15 MeV. Above 15 MeV, the ^{59}Co(n, 2n)^{58}Co reaction cross section increases slowly with neutron energy. Similarly, sharp increase of (n, 2n) reaction cross section of ^{44}Sc and ^{55}Mn within the neutron energies of 10–14 MeV and near constant value above 14 MeV was shown by Bostan and Qaim [5], which supports our present observation. On the other hand, it was observed by Qaim [3] that if the value of (N-Z)/A is greater than 0.1, then the (n, 2n) reaction cross section increases gradually around the neutron energy of 14–15 MeV. More probably, this is the reason for near constant value of ^{59}Co(n, 2n)^{58}Co reaction cross section above 15 MeV as seen from Figures 1 and 2. Besides this, opening of other reaction channels may also cause the gradual increase or near constant value of (n, 2n) reaction cross section within 14–20 MeV neutron energy. This observation indicates the partitioning of the excitation energy in different reaction channels.

5 Conclusion

The ^{59}Co(n, $2n$)^{58}Co reaction cross section at the effective neutron energies E_n = 11.98 and 15.75 MeV has been determined by using the activation method and off-line gamma ray spectrometric technique. The covariance analysis in the uncertainty of the reaction cross section has been performed by taking into account every source of error and considering the correlations between the attributes influencing the experimental data. We also provide table of partial uncertainties data required for a comprehensive compilation in the IAEA EXchange FORmat (EXFOR) database [43]. The ^{59}Co(n, $2n$)^{58}Co reaction cross section at the neutron energy of 11.98 MeV is found to be in agreement with the evaluated data, but at effective neutron energy of 15.75 MeV it is found to be slightly lower than the evaluated data. It was also found that the ^{59}Co(n, $2n$)^{58}Co reaction cross section increases from threshold energy to the neutron energy of 14–15 MeV and therefter increases very slowly or remains nearly constant up to the neutron energy of 20–21 MeV, which may be due to the partitioning of the excitation energy in different reaction channels.

Acknowledgements: One of the authors, Santhi Sheela, thanks Department of Atomic Energy-Board of Research in Nuclear Sciences (DAE-BRNS), Mumbai for the financial support through a research project (Sanction No. 36(6)/14/52/2014-BRNS/2708). The authors would like to thank Tim Vidmar, Belgian Nuclear Research Centre (SCK · CEN), Belgium for providing EFFTRAN software for calculating the correction factor due to coincidence summing. The authors would also like to thank Vinay Madhusudanan, Asst. Prof. Department of Mathematics, MIT, Manipal for his association in developing a Matlab code for computing covariance matrix. The authors are thankful to Naohiko Otsuka, International Atomic Energy Agency for his valuable expert opinion on the method of retrieving monitor cross section from IRDFF. They are also grateful to the staff of Pelletron facility, TIFR for giving the proton beam during the irradiation.

References

1. Ganesan, S.: Nuclear data requirements for accelerator driven sub-critical systems – a roadmap in the Indian context. Pramana **68**(2), 257 (2007).
2. Qaim, S.: Radiochemical determination of nuclear data for theory and applications. J. Radioanal. Nucl. Chem. **284**(3), 489 (2010).
3. Qaim, S.: Activation cross sections, isomeric cross-section ratios and systematics of (n, 2n) reactions at 14–15 MeV. Nucl. Phys. A **185**(2), 614 (1972).
4. Sudar, S., Qaim, S.: Isomeric cross-section ratio for the formation of ^{58m,g}Co in neutron, proton, deuteron, and alpha-particle induced reactions in the energy region up to 25 MeV. Phys. Rev. C **53**(6), 2885 (1996).
5. Bostan, M., Qaim, S.: Excitation functions of threshold reactions on ^{45}Sc and ^{55}Mn induced by 6 to 13 MeV neutrons. Phys. Rev. C **49**(1), 266 (1994).
6. Bormann, M., Seebeck, U., Voights, W., Woelfer, G.: Level densities of dome medium weight nuclei from evaporation spectra of the alpha particles from (n, alpha) reactions. Z. Naturforsch. A **21**, 988 (1966).
7. Dighe, P., Pansare, G., Sarkar, R., Bhoraskar, V.: Cross sections of (n, 2n) reactions induced by 14.7 MeV neutrons in ^{46}Ti, ^{50}Cr and ^{59}Co. Indian J. Pure Appl. Phys. **29**(10), 665 (1991).
8. Garlea, I., Garlea, C., Dobrea, D., Roth, C., Rosu, H. N., Rapeanu, S.: Cross sections of some reactions induced by 14 MeV neutrons. Revue Roumaine de Physique **30**(8), 673 (1985).
9. Ghorai, S., Gaiser, J., Alford, W.: The (n, 2n) isomeric cross section ratios and the (n, 2n) and (n, α) excitation functions for ^{59}Co. Ann. Nucl. Energy **7**(1), 41 (1980).
10. Greenwood, L. R.: Recent research in neutron dosimetry and damage analysis for materials irradiations. In: Influence of Radiation on Material Properties: 13th International Symposium (Part II) (1987), ASTM International, Philadelphia, p. 743.
11. Hasan, S., Pavlik, A., Winkler, G., Uhl, M., Kaba, M.: Precise measurement of cross sections for the reactions ^{59}Co(n, 2n)$^{58m+g}$Co and ^{59}Co (n, p)^{59}Fe around 14 MeV. J. Phys. G: Nucl. Phys. **12**(5), 397 (1986).
12. Iwasaki, S., Matsuyama, S., Ohkubo, T., Fukuda, H., Sakuma, M., Kitamura, M.: Measurement of activation cross-sections for several elements between 12 and 20 MeV. Vol. 1. p. 305. (No. CONF-940507) American Nuclear Society, Inc., La Grange Park, IL (United States), (1994).
13. Kimura, I., Kobayashi, K.: Calibrated fission and fusion neutron fields at the Kyoto University Reactor. Nucl. Sci. Eng. **106**(3), 332 (1990).
14. Majerle, M., Bém, P., Novák, J., Šimečková, E., Štefánik, M.: Au, Bi, Co and Nb cross-section measured by quasimonoenergetic neutrons from p + ^{7}Li reaction in the energy range of 18–36 MeV. Nucl. Phys. A **953**, 139 (2016).
15. Mannhart, W., Schmidt, D.: Measurement of neutron activation cross sections in the energy range from 8 MeV to 15 MeV. In. Physikalisch-Technische Bundesanstalt (PTB-N-53), (2007).
16. Meadows, J., Smith, D., Bretscher, M., Cox, S.: Measurement of 14.7 MeV neutron-activation cross sections for fusion. Ann. Nucl. Energy **14**(9), 489 (1987).
17. Molla, N., Miah, R., Basunia, S., Hossain, S., Rahman, M.: Cross sections of (n, p), (n, α), and (n, 2n) processes on scandium, vanadium, cobalt, copper and zinc isotopes in the energy range 13.57–14.71 MeV. Vol. 2. p. 938. (No. CONF-940507) American Nuclear Society, Inc., La Grange Park, IL (United States), (1994).
18. Osman, K. T., Habbani, F. I.: Measurement and study of (n, p) reaction cross-sections for Cr, Ti, Ni, Co, Zr and Mo isotopes using 14.7 MeV neutrons. International Atomic Energy Agency (IAEA) No. INDC (SUD)–001 (1996).
19. Ryves, T., Kolkowski, P., Judge, S.: Cobalt cross sections for 14 MeV neutrons. Ann. Nucl. Energy **15**(12), 561 (1988).

20. Semkova, V., Avrigeanu, V., Glodariu, T., Koning, A., Plompen, A., Smith, D., Sudar, S.: A systematic investigation of reaction cross sections and isomer ratios for neutrons up to 20 MeV on Ni-isotopes and ^{59}Co by measurements with the activation technique and new model studies of the underlying reaction mechanisms. Nucl. Phys. A **730**(3), 255 (2004).
21. Suita, J. C., da Silva, A. G., Auler, L. T., de Barros, S.: Neutron-induced reaction cross sections between 9 and 14 MeV. Nucl. Sci. Eng. **126**(1), 101 (1997).
22. Uno, Y., Uwamino, Y., Soewarsono, T. S., Nakamura, T.: Measurement of the neutron activation cross sections of ^{12}C, ^{30}Si, ^{47}Ti, ^{48}Ti, ^{52}Cr, ^{59}Co, and ^{58}Ni between 15 and 40 MeV. Nucl. Sci. Eng. **122**(2), 247 (1996).
23. Ganesan, S.: Nuclear data covariances in the indian context–progress, challenges, excitement and perspectives. Nucl. Data Sheets **123**, 21 (2015).
24. Chadwick, M., Herman, M., Obložinský, P., Dunn, M. E., Danon, Y., Kahler, A., Smith, D. L., Pritychenko, B., Arbanas, G., Arcilla, R., Brewer, R., Brown, D. A., Capote, R., Carlson, A. D., Cho, Y. S., Derrien, H., Guber, K., Hale, G. M., Hoblit, S., Holloway, S., Johnson, T. D., Kawano, T., Kiedrowski, B. C., Kim, H., Kunieda, S., Larson, N. M., Leal, L., Lestone, J. P., Little, R. C., McCutchan, E. A., MacFarlane, R. E., MacInnes, M., Mattoon, C. M., McKnight, R. D., Mughabghab, S. F., Nobre, G. P. A., Palmiotti, G., Palumbo, A., Pigni, M. T., Pronyaev, V. G., Sayer, R. O., Sonzogni, A. A., Summers, N. C., Talou, P., Thompson, I. J., Trkov, A., Vogt, R. L., van der Marck, S. C., Wallner, A., White, M. C., Wiarda, D., Young, P. G.: ENDF/B-VII.1 Nuclear data for science and technology: cross sections, covariances, fission product yields and decay data. Nucl. Data Sheets **112**(12), 2887 (2011).
25. Ge, Z., Zhao, Z., Xia, H., Zhuang, Y., Liu, T., Zhang, J., Wu, H.: The updated version of Chinese Evaluated Nuclear Data Library (CENDL-3.1). J. Korean Phys. Soc **59**(2), 1052 (2011).
26. Zabrodskaya, S. V., Ignatyuk, A. V., Koscheev, V. N., Manochin, V. N., Nikolaev M. N., Pronyaev, V. G. ROSFOND – Rossiyskaya Natsionalnaya Biblioteka Nejtronnykh Dannykh, VANT, Nuclear Constants 1–2, 3 (2007).
27. Shibata, K., Iwamoto, O., Nakagawa, T., Iwamoto, N., Ichihara, A., Kunieda, S., Chiba, S., Furutaka, K., Otuka, N., Ohasawa, T., Murata, T., Matsunobu, H., Zukeran, A., Kamada, S., Katakura, J.-I.: JENDL-4.0: a new library for nuclear science and engineering. J. Nucl. Sci. Technol. **48**(1), 1 (2011).
28. Koning, A., Bauge, E., Dean, C., Dupont, E., Fischer, U., Forrest, R., Jacqmin, R., Leeb, H., Kellett, M., Mills, R.: Status of the JEFF nuclear data library. J. Korean Phys. Soc **59**(2), 1057 (2011).
29. Koning, A. J., Rochman, D., Kopecky, J., Sublet, J. C., Fleming, M., Bauge, E., Hilaire, S., Romain, P., Morillon, B., Duarte, H., Marck, S. C. V., Pomp, S., Sjostrand, H., Forrest, R., Henriksson, H., Cabellos, O., Goriely, S., Leppanen, J., Leeb, H., Lompen, A., Mills, R.: TENDL-2015: TALYS-based evaluated nuclear data library. Available at: https://tendl.web.psi.ch/tendl_2015/tendl2015.html (2015).
30. Capote, R., Zolotarev, K. I., Pronyaev, V. G., Trkov, A.: Updating and extending the IRDF-2002 dosimetry library. J. ASTM Int. **9**(4), 1 (2012).
31. Ziegler, J. F., Ziegler, M. D., Biersack, J. P.: SRIM–The stopping and range of ions in matter. Nucl. Instrum. Methods Phys. Res. B **268**(11–12), 1818 (2010). Available at: http://www.srim.org/.
32. Badwar, S., Ghosh, R., Lawriniang, B. M., Vansola, V., Sheela, Y. S., Naik, H. Naik, Y., Suryanarayana, S. V., Jyrwa, B., Ganesan, S.: Measurement of formation cross-section of ^{99}Mo from the ^{98}Mo(n,γ) and ^{100}Mo(n,2n) reactions. Appl. Radiat. Isot. **129**, 117 (2017).
33. Yerraguntla, S. S., Naik, H., Karantha, M. P., Ganesan, S., Suryanarayana, S. V., Badwar, S.: Measurement of ^{59}Co(n, γ)^{60}Co reaction cross sections at the effective neutron energies of 11.98 and 15.75 MeV. J. Radioanal. Nucl. Chem. **314**(1), 457 (2017).
34. Sonzogni, A.: NuDat 2.7β (2017), National Nuclear Data Center, Brookhaven National Laboratory. http://www.nndc.bnl.gov/.
35. Smith, D. L., Plompen, A. J. M., Semkova, V.: Correction for low energy neutrons by spectral indexing, vol. 75. Organisation for Economic Co-Operation and Development-Nuclear Energy Agency (NEA/WPEC-19, ISBN 92-64-01070-X), Paris (France), (2005).
36. Millsap, D., Landsberger, S.: Self-attenuation as a function of gamma ray energy in naturally occurring radioactive material in the oil and gas industry. Appl. Radiat. Isot. **97**, 21 (2015).
37. Nowotny, R.: XMuDat: Photon attenuation data on PC. In: IAEA Report IAEA-NDS, vol. 195 (1998).
38. Santhi Sheela, Y., Naik, H., Manjunatha Prasad, K., Ganesan, S., Sreekumaran Nair, N., Suryanarayana, S. V.: The efficiency and error covariance matrix of HPGe detector at characteristic gamma energies of reaction products ^{58}Co and ^{115m}In in the measurement of ^{59}Co(n, 2n)^{58}Co reaction cross section relative to ^{115}In(n, n′)^{115m}In Internal Report No. MU/STATISTICS/DAE-BRNS/2017/2, March-2017, DOI: 10.13140/RG.2.2.28301.95206 (2017).
39. Santhi Sheela, Y., Naik, H., Manjunatha Prasad, K., Ganesan, S., Sreekumaran Nair, N., Suryanarayana, S. V.: Covariance analysis of efficiency calibration of HPGe detector. Internal Report, No. MU/STATISTICS/DAE-BRNS/2017/1, 19-February-2017, DOI: 10.13140/RG.2.2.32025.21605 (2017).
40. Smith, D.: On the relationship between micro and macro correlations in nuclear measurement uncertainties. Nucl. Instr. Methods Phys. Res. A **257**(2), 365 (1987).
41. Koning, A., Rochman, D., van der Marck, S., Kopecky, J., Sublet, J., Pomp, S., Sjostrand, H., Forrest, R.: TALYS Evaluated Nuclear Data Library (TENDL-2015). Nuclear Research and Consultancy Group (NRG) Petten, The Netherlands (2015).
42. Evaluated Nuclear Data File ENDF/B-VII.1. https://www-nds.iaea.org/exfor/endf.htm (2011).
43. Otuka, N., Dupont, E., Semkova, V., Pritychenko, B., Blokhin, A. I., Aikawa, M., Babykina, S., Bossant, M., Chen, G., Dunaeva, S., Forrest, R. A., Fukahori, T., Furutachi, N., Ganesan, S., Ge, Z., Gritzay, O. O., Herman, M., Hlavac, S., Kato, K., Lalremruata, B., Lee, Y. O., Makinaga, A., Matsumoto, K., Mikhaylyukova, M., Pikulina, G., Pronyaev, V. G., Saxena, A., Schwerer, O., Simakov, S. P., Soppera, N., Suzuki, R., Takacs, S., Tao, X., Taova, S., Tarkanyi, F., Varlamov, V. V., Wang, J., Yang, S. C., Zerkin, V., Y, Z.: Towards a more complete and accurate experimental nuclear reaction data library (EXFOR): international collaboration between nuclear reaction data centres (NRDC). Nuclear Data Sheets **120**, 272 (2014).